JOURNAL OF SOLID STATE CHEMISTRY 109, 315–320 (1994)

(Tetrakis(2-pyridylmethyl)ethylenediamine)iron(II) Perchlorate. Phase Transition Study about the First Rapidly Interconverting Ferrous Spin-Crossover Complex

Xavier Solans[1]

[1]*Departament Cristallografia, Mineralogia i Dipòsits Minerals, Universitat de Barcelona, 08028-Barcelona, Spain*

Lena Ruiz-Ramirez and Rafael Moreno-Esparza

Departamento Química Inorgánica, UNAM, México D.F., México

Manuel Labrador

Departament Cristallografia, Mineralogia i Dipòsits Minerals, Universitat de Barcelona, 08028-Barcelona, Spain

and

Albert Escuer

Departament Química Inorgánica, Universitat de Barcelona, 08028-Barcelona, Spain

Received December 10, 1992; in revised form August 3, 1993; accepted August 3,1993

A detailed variable-temperature magnetic, thermal and single-crystal and powder diffractometry study has been made on $[Fe(tpen)](ClO_4)_2 \cdot \frac{1}{2}H_2O$. (tpen = tetrakis(2-pyridylmethyl)ethylenediamine.) Solid-state magnetic susceptibilities measurement shows that this complex is a continuous/complete type Fe^{II} spin-crossover system as defined by Gütlich, with an effective critical temperature, T_c, where there are equal amounts of high- and low-spin complexes, equal to 365 K. The ^{57}Fe Mössbauer spectrum measured by Hendrickson shows that the interconversion rate between high- and low-spin states is faster than the Mössbauer time scale. Single-crystal diffractometry shows that the $[Fe(tpen)](ClO_4)_2 \cdot \frac{1}{2}H_2O$ crystallizes in the monoclinic space group $C2/c$, which at 293 K has a unit cell of $a = 40.775(8)$ Å, $b = 9.467(2)$ Å, $c = 23.851(5)$ Å, and $\beta = 108.32(6)°$ with $Z = 12$, and at 182 K has a unit cell of $a = 40.430(3)$ Å, $b = 9.460(1)$ Å, $c = 23.834(2)$, Å, and $\beta = 108.59(2)°$ with $Z = 12$. The refinements were carried out with 3228 and 3639 (2.5σ) observed reflections at 293 and 182 K, respectively, to give $R = 0.058$ ($wR = 0.061$) and $R = 0.032$ ($wR = 0.036$). At both temperatures there are two crystallographically different $[Fe(tpen)]^{+2}$ cations, showing an octahedral coordination strongly distorted to trigonal geometry by the steric constraints produced by the hexadentate ligand. This distortion is different in the two nonequivalent cations, which is due to different intermolecular interaction produced by the perchlorate anions. An analysis of the changes in the structure of the two cations as a function of temperature from our results and those obtained by Hendrickson shows that the two cations act independently in the interconversion procedure. DSC thermal analysis shows low and broadening maxima in the cooling and warming process, and a thermal hysteresis which is due to the fast rate of spin-state interconversion. Variable-time cycles studied by powder X-ray diffraction show a variation of preferred orientation during the cooling and warming process, and a variation of the results according to the elapsed-time, slow procedure (period of 140 min) shows a reversible equilibrium transition without thermal hysteresis, while a shorter period (30 min) shows a delay in the spin interconversion.

INTRODUCTION

The temperature-dependent low-spin ($^1A_1$) → high-spin ($^5T_2$) transitions in iron(II) complex compounds have been a subject of extensive interest within recent years. Apart from a few examples all the investigated systems are with di-, tetra-, or hexaimine ligands. Multidentate ligands are especially desirabel in order to enhance the stability of the complex in solution and to ensure that the magnetic properties of the iron(II) complexes in solid state reflect the molecular spin-equilibrium phenomena more than collective spin-phase transitions in the lattice.

Toftlund and Yde-Andersen (1) and Chang and *et al.* (2) have studied the preparation and characterization of the Fe^{II} spin-crossover complex (tetrakis(2-pyridylmethyl)ethylenediamine) iron(II). The second group re-

[1] To whom correspondence should be addressed.

0022-4596/94 $6.00

ported the crystal structure determination at 298 and 358 K, solid-state magnetic susceptibility data, ^{57}Fe Mössbauer spectra and variable-temperature ^1H NMR data; they concluded that the dynamics of this complex are little affected by intermolecular interactions, and that this complex interconverts in the solid state at a rate that is faster than the time scale of the Mössbauer experiment.

In order to get a better understanding of the interconversion process, crystal structure determination at 293 and 182 K (the second temperature has been selected because low-spin state is expected according to magnetic susceptibility measurements), DSC analysis, and variable-temperature and -time powder X-ray diffraction have been carried out; these show that the two crystallographically nonequivalent molecules act in a different way during the Fe^{II} spin crossover, explaining the long temperature range observed from solid-state magnetic susceptibility measurements and DSC analysis. Moreover, a study on the thermal hysteresis and the time-rate interconversion has been carried out.

TABLE 1
Crystallographic Data for $[Fe(tpen)](ClO_4)_2 \cdot \frac{1}{2}H_2O$

	T (K)	
	182	293
Formula	$FeCl_2O_{8.5}N_6C_{26}H_{29}$	
Formula wt	683.308	
Crystal size (mm)	0.1 × 0.1 × 0.2	0.1 × 0.1 × 0.2
Space group	$C2/c$ (No. 15)	
a (Å)	40.430(3)	40.775(8)
b (Å)	9.460(1)	9.467(2)
c (Å)	23.834(2)	23.851(5)
β (°)	108.59(2)	108.32(6)
V (Å^3)	8640(2)	8740(5)
Z	12	
ρ_{calc} (g cm^{-3})	1.587	1.569
λ ($K\alpha$) (Å)	0.71069	
2θ range (°)	4.0–50.0	
Octants collected	$\pm h, +k, +l$	
R_{int} (on F)	0.019	0.042
Total reflections	7321	7319
Observed reflections ($I > 2.5\sigma(I)$)	3639	3228
μ (cm^{-1})	7.88	7.79
R^a	0.032	0.058
wR^b	0.036	0.061

[a] $R = \Sigma(|F_o| - |F_c|)/\Sigma|F_o|$.
[b] $wR = \Sigma w(|F_o| - |F_c|)/\Sigma w|F_o|$.

EXPERIMENTAL

Compound preparation. All reagents were commercially available and used without further purification. All synthetic procedures involving Fe^{II} complexes were performed under an inert Ar atmosphere, using standard Schlenk techniques.

The tetrakis(2-pyridylmethyl)ethylenediamine (tpen) was prepared by reaction of the diamines with an excess of (2-pyridylmethyl)chloride in ethanol. The free base was purified by crystallization from petroleum ether. The perchlorate of the iron(II) complex was obtained in high yields from aqueous iron(II) perchlorate solutions by addition of the equimolar amounts of the free bases. Crystals were obtained by slow evaporation from aqueous solution. Analysis calculated for $FeC_{26}H_{29}N_6O_{8.5}Cl_2$: C, 45.37; H, 4.25; N, 12.21; Fe, 8.11; found: C, 45.35; H, 4.21; N, 12.19; Fe, 8.12.

Physical measurement. Magnetic susceptibilities were measured with a Faraday-type magnetometer (Manics DMS8) equipped with an Oxford helium continuous-flow cryostat and a Drusch EAF 16UE electromagnet. The magnetic field was approximately 15,000 G. Diamagnetic corrections were estimated by Pascal tables.

DSC analysis. Thermal characterization was carried out using a Perkin–Elmer, model DSC-7, differential scanning calorimeter with the required cryogenic equipment. The sample weight was 1.649 mg. A heating rate of 5°C/min and a total scale sensitivity of 0.4 mW were used.

X-ray structure determination. Diffraction data were collected on an Enraf–Nonius CAD4 automated diffractometer equipped with a graphite monochromator. The ω-Θ scan technique was used to record the intensities for all nonequivalent reflections. The scan widths were calculated as $A + B \tan \Theta$, where A is estimated from the mosaicity of the crystal and B allows for the increase in peak width due to Mo$K\alpha_1$–$K\alpha_2$ splitting.

Six different crystals were used for independent intensity data collection. Here we give the result of the best successful refinement at 293 and 182 K. The differences obtained in the different crystal structure refinement are in the range of two times the standard deviation.

Pertinent details regarding the structure determination are listed in Table 1 for both structures. The unit-cell parameters were obtained by a least-squares fit to the automatically centered settings from 25 reflections. The space group was based upon the successful refinement of the proposed model in the centric space group. The intensities from three control reflections for each measurement showed no significant fluctuation during the data collection. Intensity data for both structures were corrected for Lorentz and polarization effects, as well as anomalous dispersion effects. Absorption corrections were not applied.

Both structures were solved by direct methods, using the SHELX-86 computer program (3), and refined by full-matrix least-squares method, using the SHELX-76 computer program (4). The function minimized was $w||F_o| - |F_c||^2$, where the weighting scheme was $w = (\sigma^2(F_o) + k|F_o|^2)^{-1}$. Disordered oxygen atoms for perchlorate ions C1(2) and C1(3) at 293 K were obtained from a difference synthesis. The positions of hydrogen atoms were

computed and refined with an overall isotropic temperature factor, using a riding model.

In all crystal structure determinations, using different crystals, one position assignable as hydrate water molecule was obtained in the Fourier synthesis. The final difference Fourier map had no significant features, and final analysis of variance between observed and calculated structure factors does not show apparent systematic errors; thereby, we assume a formula of the compound with $\frac{1}{2}$ H_2O, while Toftlund and Yde-Andersen (1) assigned one H_2O, and Chang and *et al.* (2) $\frac{2}{3}$.

X-Ray powder diffraction. Powder diffraction data were collected with a Siemens D500 automated diffractometer, using Cu$K\alpha$ radiation and a secondary monochromator. Three different procedures were carried out. The first consists of a cycle of cooling and warming process with a rate of 10°C/min, and leaving the sample for ten minutes at measuring temperature, in order to stabilize the equipment and the sample. Intensity data were measured at 223, 248, 273, 293, 323, 383, and 423 K. The second consists of three cycles of cooling and warming processes with a rate of 10°C/min and the same restoring time. Intensity data only were measured at 223 and 423 K. The difference between the two procedures is the elapsed time in the intensity collection at the same temperature, 140 and 30 min, respectively. In the third procedure, intensities were collected at 293 K, following the previous cycling, each 60 min.

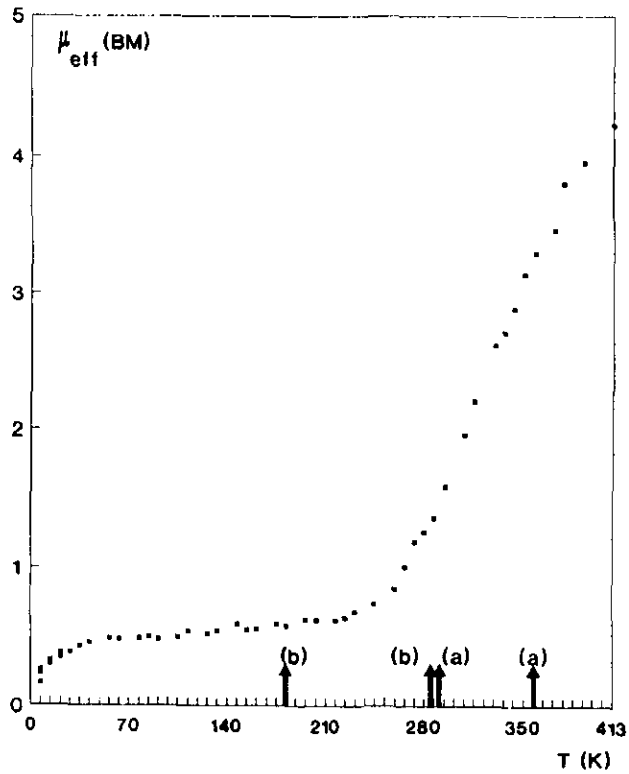

FIG. 1. Temperature dependence of the effective magnetic moments μ_{eff} and temperature where crystal structure has been determined. (a) Chang *et al.* (2) and (b) this work.

RESULTS AND DISCUSSION

X-Ray crystal structure of $[Fe(tpen)](ClO_4)_2 \cdot \frac{1}{2}H_2O$. We solved the crystal structure of the title compound at 182 and 293 K in order to determine the variation of the geometric values according to the temperature, and compared our results with those obtained by Chang *et al.* (2) at 298 and 358 K (Fig. 1). The first problem was that our crystallization process gave only $\frac{1}{2}$ water molecule, in contrast to the $\frac{2}{3}$ obtained by the preceding authors. This fact could explain the significant difference between the cell parameters at 293 and 298 K [**a** = 40.775, **b** = 9.467, and **c** = 23.851 Å for $\frac{1}{2}$ H_2O at 293 K, and **a** = 40.87, **b** = 9.497, and **c** = 23.946 for $\frac{2}{3}$ H_2O at 298 K], but we return to this discussion when we give the results from X-ray diffraction on powder samples, and consider determinations similar to the two crystal structure determinations according to the magnetic and X-ray crystal structure results.

Selected bond distances and angles are listed in Table 2; a plot of Fe(tpen) is given in Fig. 2 with the numbering of atoms. Crystallographically, the cation occupies two different sites in the lattice. Each nonequivalent symmetry Fe ion is surrounded by six N atoms, two of which belong to the ethylenediamine moiety and the remaining four to the same number of methylpiridinium moieties of the same ligand. We consider as the equatorial plane in our discussion the one defined by the two aliphatic nitrogen and two pyridinium N atoms, while the remaining pyridinium N atoms occupy the apical sites.

Both Fe ions show a distorted octahedral coordination polyhedron, which is due to short N(et)–Fe–N(et) [87.3° at 182 K and 86.0° at 293 K] and N*(py)–Fe–N(et) [83.0° at 182 K and 82.6° at 293 K] bond angles [where N*(py) specifies a nitrogen atom belonging to a methylpiridinium linked at N(et)]. This fact produces an increase in the remaining N(py)–Fe–N(et) angles and in the separation between the two N(1), N(8), N(15), and N(1′), N(8′), N(15′) trigonal faces of the Fe(1) octahedron and the N(16), N(26), N(33), and N(19), N(40), N(47) trigonal faces of the Fe(2) octahedron, which facilitates the octahedron distortions due to intermolecular forces. The mean twist angle between the above-defined trigonal faces is equal to 55.6° (182 K) and 56.82° (293 K) for Fe(1), and 48.5° (182 K) and 46.3° (293 K) for the Fe(2) polyhedron, which is expected to be 60° for a strictly octahedral polyhedron. So, the Fe(1) ion shows a closer octahedral coordination than the Fe(2) ion. The differences between the Fe(1) and Fe(2) polyhedra are explained by the intermolecular interaction between the Fe(tpen) and the perchlo-

TABLE 2
Selected Bond Distances and Angles for [Fe(tpen)]ClO) · ½HO

	T (K)			T (K)	
	182	293		182	293
		Distances (Å)			
N(16)–Fe(2)	1.933(1)	2.012(7)	N(40)–C(35)	1.436(2)	1.36(1)
N(19)–Fe(2)	2.005(1)	2.028(10)	C(37)–C(36)	1.388(3)	1.39(2)
N(26)–Fe(2)	2.006(1)	2.011(9)	C(38)–C(37)	1.433(2)	1.37(2)
N(33)–Fe(2)	2.006(1)	2.028(8)	C(39)–C(38)	1.471(2)	1.33(1)
N(40)–Fe(2)	1.987(1)	1.988(7)	N(40)–C(39)	1.191(2)	1.35(1)
N(47)–Fe(2)	2.013(1)	2.023(7)	C(42)–C(41)	1.474(3)	1.48(1)
C(17)–N(16)	1.635(3)	1.47(2)	C(43)–C(42)	1.382(2)	1.37(1)
C(20)–N(16)	1.541(2)	1.49(1)	N(47)–C(42)	1.381(2)	1.34(1)
C(27)–N(16)	1.520(2)	1.52(1)	C(44)–C(43)	1.416(3)	1.38(2)
C(18)–C(17)	1.591(2)	1.50(1)	C(45)–C(44)	1.371(3)	1.38(2)
N(19)–C(18)	1.469(2)	1.49(1)	C(46)–C(45)	1.427(2)	1.36(1)
C(34)–N(19)	1.430(2)	1.48(1)	N(47)–C(46)	1.319(2)	1.31(1)
C(41)–N(19)	1.580(2)	1.50(1)	N(1)–Fe(1)	2.012(1)	1.988(8)
C(21)–C(20)	1.507(3)	1.48(2)	N(8)–Fe(1)	1.960(1)	1.966(8)
C(22)–C(21)	1.442(2)	1.36(2)	N(15)–Fe(1)	1.985(2)	1.985(7)
N(26)–C(21)	1.380(1)	1.35(1)	C(1)–N(1)	1.483(2)	1.48(1)
C(23)–C(22)	1.164(4)	1.38(2)	C(2)–N(1)	1.483(2)	1.49(2)
C(24)–C(23)	1.509(3)	1.37(2)	C(9)–N(1)	1.574(2)	1.48(1)
C(25)–C(24)	1.449(2)	1.35(2)	C(1)–C(1)	1.752(4)	1.52(3)
N(26)–C(25)	1.254(2)	1.32(1)	C(3)–C(2)	1.515(2)	1.49(1)
C(28)–C(27)	1.459(2)	1.46(2)	C(4)–C(3)	1.387(2)	1.34(2)
C(29)–C(28)	1.437(2)	1.41(2)	N(8)–C(3)	1.329(2)	1.35(1)
N(33)–C(28)	1.332(1)	1.34(1)	C(5)–C(4)	1.387(2)	1.34(2)
C(30)–C(29)	1.284(3)	1.34(2)	C(6)–C(5)	1.346(2)	1.40(2)
C(31)–C(30)	1.447(2)	1.38(2)	C(7)–C(6)	1.362(2)	1.36(2)
C(32)–C(31)	1.351(2)	1.36(2)	N(8)–C(7)	1.400(2)	1.36(1)
N(33)–C(32)	1.422(2)	1.37(1)	C(10)–C(9)	1.456(2)	1.51(2)
C(35)–C(34)	1.437(2)	1.48(1)	C(11)–C(10)	1.364(2)	1.37(1)
C(36)–C(35)	1.318(2)	1.34(1)	N(15)–C(14)	1.319(2)	1.36(1)
		Angles (°)			
N(19)–Fe(2)–N(16)	87.3(1)	85.7(3)	C(32)–N(33)–Fe(2)	125.5(1)	126.7(6)
N(26)–Fe(2)–N(16)	82.0(1)	80.8(3)	C(32)–N(33)–C(28)	117.6(1)	118.2(8)
N(26)–Fe(2)–N(19)	168.0(1)	164.6(3)	C(35)–C(34)–N(19)	111.9(1)	110.2(8)
N(33)–Fe(2)–N(16)	82.8(1)	83.6(3)	C(36)–C(35)–C(34)	124.9(2)	123.3(11)
N(33)–Fe(2)–N(19)	95.9(1)	98.6(3)	N(40)–C(35)–C(34)	115.0(1)	115.6(8)
N(33)–Fe(2)–N(26)	88.2(1)	87.5(3)	N(40)–C(35)–C(36)	120.2(2)	121.1(10)
N(40)–Fe(2)–N(16)	167.8(1)	165.8(3)	C(37)–C(36)–C(35)	120.6(2)	119.4(11)
N(40)–Fe(2)–N(19)	82.9(1)	82.5(3)	C(38)–C(37)–C(36)	121.4(1)	120.4(10)
N(40)–Fe(2)–N(26)	108.4(1)	111.8(3)	C(39)–C(38)–C(37)	109.7(1)	116.8(11)
N(40)–Fe(2)–N(33)	91.0(1)	90.3(3)	N(40)–C(39)–C(38)	129.8(1)	125.1(11)
N(47)–Fe(2)–N(16)	101.5(1)	100.8(3)	C(35)–N(40)–Fe(2)	109.5(1)	112.1(6)
N(47)–Fe(2)–N(19)	85.6(1)	83.3(3)	C(39)–N(40)–Fe(2)	132.5(1)	130.8(7)
N(47)–Fe(2)–N(26)	91.3(1)	91.7(3)	C(39)–N(40)–C(35)	118.0(1)	117.0(8)
N(47)–Fe(2)–N(33)	175.5(1)	175.3(3)	C(42)–C(41)–N(19)	110.7(2)	112.5(11)
N(47)–Fe(2)–N(40)	84.9(1)	85.7(3)	C(43)–C(42)–C(41)	119.7(2)	119.8(11)
C(17)–N(16)–Fe(2)	111.1(1)	107.9(6)	N(47)–C(42)–C(41)	118.8(1)	117.6(9)
C(20)–N(16)–Fe(2)	108.3(1)	105.0(5)	N(47)–C(42)–C(43)	121.1(2)	122.2(9)
C(20)–N(16)–C(17)	107.4(1)	113.6(8)	C(44)–C(43)–C(42)	117.3(2)	119.4(11)
C(27)–N(16)–Fe(2)	113.3(1)	110.0(6)	C(45)–C(44)–C(43)	122.2(1)	117.0(10)
C(27)–N(16)–C(17)	108.5(1)	110.6(8)	C(46)–C(45)–C(44)	116.4(2)	120.4(11)
C(27)–N(16)–C(20)	108.1(1)	109.5(8)	N(47)–C(46)–C(45)	122.4(1)	122.2(11)
C(18)–C(17)–N(16)	98.4(1)	106.7(8)	C(42)–N(47)–Fe(2)	113.1(1)	114.4(6)
N(19)–C(18)–C(17)	111.2(1)	108.9(8)	C(46)–N(47)–Fe(2)	125.2(1)	124.9(7)
C(18)–N(19)–Fe(2)	107.2(1)	105.1(6)	C(46)–N(47)–C(42)	120.2(1)	118.8(8)
C(34)–N(19)–Fe(2)	106.0(1)	104.6(7)	N(8)–Fe(1)–N(1)	81.1(1)	81.9(3)
C(34)–N(19)–C(18)	116.9(1)	116.7(7)	N(15)–Fe(1)–N(1)	96.1(1)	96.7(3)
C(41)–N(19)–Fe(2)	110.4(1)	111.1(7)	N(15)–Fe(1)–N(8)	92.6(1)	91.2(3)
C(41)–N(19)–C(18)	104.9(1)	110.9(8)	C(1)–N(1)–Fe(1)	105.9(1)	106.6(6)
C(41)–N(19)–C(34)	111.3(1)	108.3(7)	C(2)–N(1)–Fe(1)	105.4(1)	105.1(6)
C(21)–C(20)–N(16)	99.9(1)	105.8(8)	C(2)–N(1)–C(1)	110.4(2)	113.7(9)
C(22)–C(21)–C(20)	125.7(1)	123.1(9)	C(9)–N(1)–Fe(1)	109.3(1)	112.2(6)
N(26)–C(21)–C(20)	119.4(1)	116.0(10)	C(9)–N(1)–C(1)	113.0(1)	111.2(7)
N(26)–C(21)–C(22)	114.8(1)	120.8(11)	C(9)–N(1)–C(2)	112.3(1)	107.8(8)
C(23)–C(22)–C(21)	125.7(1)	118.4(10)	N(1)–Fe(1)–N(1)	87.3(1)	86.2(4)
C(24)–C(23)–C(22)	123.3(2)	120.4(12)	C(3)–C(2)–N(1)	105.2(1)	107.6(10)
C(25)–C(24)–C(23)	108.0(2)	117.6(12)	C(4)–C(3)–C(2)	120.3(1)	124.3(12)
N(26)–C(25)–C(24)	127.7(1)	123.4(9)	N(8)–C(3)–C(2)	115.5(1)	114.5(10)

TABLE 2—*Continued*

	T (K)			T (K)	
	182	293		182	293
C(21)–N(26)–Fe(2)	108.6(1)	111.8(8)	N(8)–C(3)–C(4)	124.2(1)	121.2(11)
C(25)–N(26)–Fe(2)	131.0(1)	128.9(6)	C(5)–C(4)–C(3)	117.8(2)	121.9(13)
C(25)–N(26)–C(21)	120.4(1)	119.3(9)	C(6)–C(5)–C(4)	119.1(1)	118.5(13)
C(28)–C(27)–N(16)	110.6(1)	113.3(8)	C(7)–C(6)–C(5)	121.6(1)	118.6(12)
C(29)–C(28)–C(27)	122.3(1)	119.8(9)	N(8)–C(7)–C(6)	120.7(1)	122.1(11)
N(33)–C(28)–C(27)	116.6(1)	117.4(10)	C(3)–N(8)–Fe(1)	113.6(1)	113.0(7)
N(33)–C(28)–C(29)	121.0(1)	122.8(10)	C(7)–N(8)–Fe(1)	129.7(1)	129.3(7)
C(3)–C(29)–C(28)	120.4(1)	117.7(10)	C(7)–N(8)–C(3)	116.5(1)	117.8(9)
C(31)–C(30)–C(29)	120.7(1)	120.1(12)	C(10)–C(9)–N(1)	112.2(1)	111.3(8)
C(32)–C(31)–C(30)	117.7(1)	120.8(11)	C(11)–C(10)–C(9)	122.5(1)	121.1(9)
N(33)–C(32)–C(31)	121.7(1)	120.2(9)	C(14)–N(15)–Fe(1)	123.2(1)	127.8(6)
C(28)–N(33)–Fe(2)	114.2(1)	113.6(6)			

rate ions. The number of shortest O(perchlorate) · · · H(tpen) lengths are 1 and 7 for Fe(1) and Fe(2), respectively, at 293 K, and 2 and 10, respectively, at 182 K. (We have defined as the shortest intermolecular length those distances in the range 2.3–2.5 Å.)

The different coordination lengths at different temperatures are shown in Table 3. From this table we can observe the following: (a) the Fe–N(py) bond length depends on the atom occupying the *trans*-position, being shortest when a N(a1) occupies the *trans*-position, which could indicate a π-back-donation effect by the N(py). (b) The bond lengths for Fe(1) at 182 and 293 K are similar, while Fe(2) shows shortest distances at 182 K, which shows that the two crystallographically nonequivalent Fe ions do not act simultaneously during the spin transition; a similar example was observed by Fleisch *et al.* (5). This is related to the different twist angle between trigonal faces in the Fe coordination polyhedron, and it is well known from the work of Hendrickson and co-workers (6–8) Gütlich (9), König *et al.* (10), and Kennedy *et al.* (11) that differences in coordination polyhedra can have a substantial impact in spin-crossover properties, particularly for complexes of amines. Thus, Fig. 1 must be read as the addition of two independent curves, which explains the unusually large temperature range of spin transition.

Spin-transition study. Chang *et al.* (2) studied the spin transition by ^{57}Fe Mössbauer spectroscopy, and they concluded that the transition between high- and low-spin states interconvert at a rate that is faster than the Mössbauer time scale.

DSC analysis shows low and broadening maxima, one peak during the cooling process, with a range of 194.1 K, and two maxima during the warming process, with ranges of 90.0 and 22.4 K. This makes it difficult to determine the transition energy and the transition temperature T_c. The interconversion starts during the cooling process at 373.6 K, and ends at 240 K, while the two maxima in the warming process have ranges of 273–360 and 365–387 K.

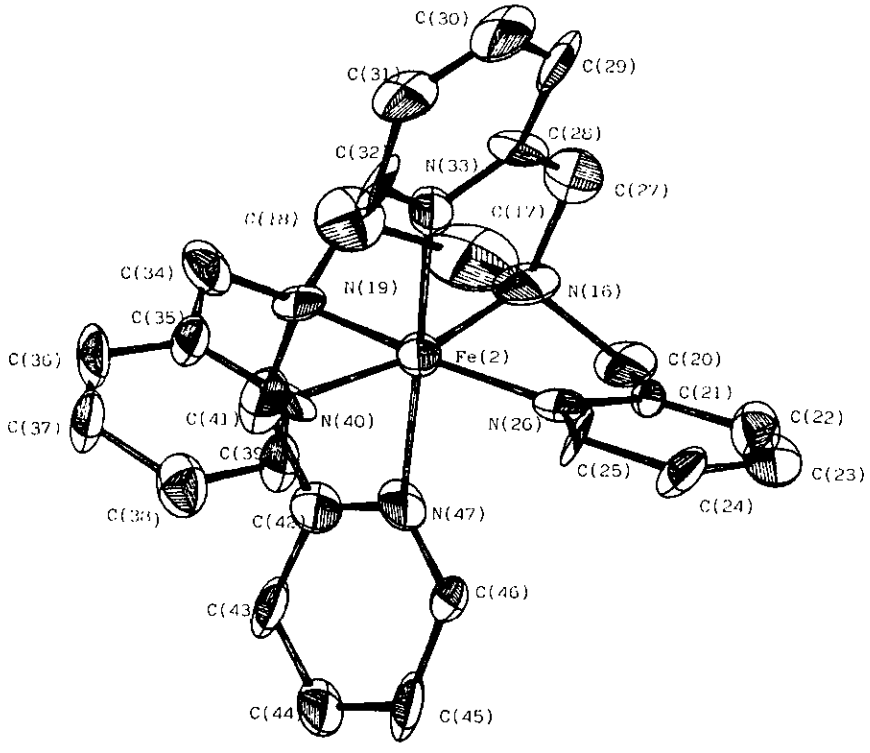

FIG. 2. ORTEP drawing of the $[Fe(tpen)]^{2+}$ cation, with the numbering scheme.

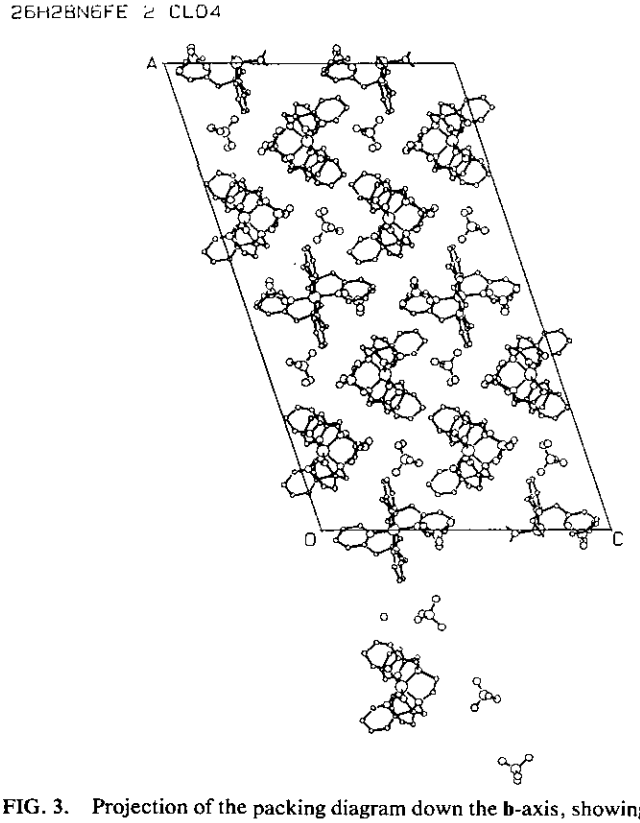

FIG. 3. Projection of the packing diagram down the **b**-axis, showing the different relative position of the ClO_4 anion with respect to the two different cations.

The broadening of the maximum supports our conclusion drawn from the result obtained by single-crystal X-ray diffraction, that the two Fe ions act independently in the spin interconversion. The asymmetry between the cooling and warming processes suggests a thermal hysteresis due to the existence of a gap energy in the interconversion process. Therefore, a study of the powder diffraction as a function of time has been carried out.

Two facts are observed in the low-speed process: (a) The preferred orientation of the sample changes with temperature, indicated by the large variation of observed intensity data. The (101) preferred orientation appears at low temperature (223 K), and the (100) orientation at high temperature (473 K). This variation can be produced by a change in the morphology of the crystals or by a reorientation of the crystals in the holder. (b) The cell parameters determined at a temperature are independent of the process followed to obtain this temperature (a warming or a cooling process); therefore, we conclude that the thermal hysteresis observed by DSC analysis is due to an inertia of the material to spin interconversion, which corroborates the results of Chang *et al.*, (2) observed from ^{57}Fe Mössbauer, or of Toftlund *et al.*, observed from magnetic susceptibility measurements. Moreover, the cell parameters determined at 293 K have, within the standard deviation range, the same values as those obtained by us from a single-crystal diffractometry.

TABLE 3
Mean Fe Coordination Bond Distance at Different Temperatures

	T (K)			
	182 (a)	293 (a)	298 (b)	358 (b)
Fe(1)–N(al)	2.012	1.988	2.000	2.09
Fe(1)–N(py,eq)	1.960	1.966	1.967	2.02
Fe(1)–N(py,ap)	1.985	1.985	1.996	2.10
Fe(2)–N(al)	1.969	2.020	2.044	2.09
Fe(2)–N(py,eq)	1.996	2.000	2.000	2.01
Fe(2)–N(py,ap)	2.009	2.026	2.033	2.06

Note. (a) From this work and (b) from Chang *et al.* (2).

When the powder diffraction process time is shortened (procedures 2 and 3) the cell parameters increase with the number of cycles. Thus, the cell volume is equal to 8631(7) $Å^3$ at 223 K in the first cycle and 8700(7) after three cycles (8773(7)–8811(7) at 293 K and 9090(7)–9123(7) at 423 K). The increase of the cell parameters indicates a delay in the spin interconversion, when the procedure is cycled with short periods. The different behavior according to the time of the cooling process suggests that the best X-ray structure determination is obtained when the single crystal is cooled more slowly, as was found from the different crystal structure determination at low temperature.

REFERENCES

1. H. Toftlund and S. Yde-Andersen, *Acta Chem. Scand., Ser. A* **35,** 575 (1981).
2. H-R. Chang, J. K. McCusker, H. Toftlund, S. R. Wilson, A. X. Trautwein, H. Winkler, and D. N. Hendrickson, *J. Am. Chem. Soc.* **112,** 6814 (1990).
3. G. M. Sheldrick, *Acta Crystallogr., Sect. A* **46,** 467 (1990).
4. G. M. Sheldrick, "SHELX. A computer program for crystal structure determination." Univ. of Cambridge, 1976.
5. J. Fleisch, P. Gütlich, K. M. Hasselbach, and W. Müller, *Inorg. Chem.* **15,** 958 (1976).
6. W. D. Federer and D. N. Hendrickson, *Inorg. Chem.* **23,** 3870 (1984).
7. M. S. Haddad, M. W. Lynch, W. D. Federer, and D.N. Hendrickson, *Inorg. Chem.* **20,** 123 (1981).
8. M. S. Haddad, W. D. Federer, M. W. Lynch, and D. N. Hendrickson, *Inorg. Chem.* **20,** 131 (1981).
9. P. Gütlich, *Struct. Bonding (Berlin)* **44,** 83 (1981).
10. E. König, G. Ritter, S.K. Kulshreshtha, and S. M. Nelson, *J. Am. Chem. Soc.* **105,** 1924 (1983).
11. B. J. Kennedy, A. C. McGrath, K. S. Murray, B. W. Skelton, and A. H. White, *Inorg. Chem.* **26,** 483 (1987).